AD-A282 322

‖‖‖‖‖‖‖‖‖‖‖‖

Self Assembly of n-Alkanethiolate Monolayers on Silver Nano-Structures:
Determination of the Apparent Thickness of the Monolayer
by Scanning Tunneling Microscopy

by

Weinjie Li, Jorma A. Virtanen, and Reginald M. Penner

DTIC
S ELECTE
JUL 2 5 1994
F

Prepared for Publication

in the

Journal of Physical Chemistry

94-23245

‖‖‖‖‖‖‖‖‖‖‖‖

University of California, Irvine
Department of Chemistry
Irvine, CA 92717-2025

July 12, 1994

DTIC QUALITY INSPECTED 5

94   22   198

REPORT DOCUMENTATION PAGE

Public reporting burden for this collection of information is estimated to average 1 hour per response, including the time for reviewing instructions, searching existing data sources, gathering and maintaining the data needed, and completing and reviewing the collection of information. Send comments regarding this burden estimate or any other aspect of this collection of information including suggestions for reducing this burden, to Washington Headquarters Services, Directorate for Information Operations and Reports, 1215 Jefferson Davis Highway, Suite 1204, Arlington, VA 22202-4302, and to the Office of Management and Budget, Paperwork Reduction Project (0704-0188), Washington, CD 20503.

1. AGENCY USE ONLY (LEAVE BLANK)	2. REPORT DATE July 13, 1994	3. REPORT TYPE AND DATES COVERED Interim May 1993 - June 1994

4. TITLE AND SUBTITLE Self Assembly of n-Alkanethiolate Monolayers on Silver Nano-Structures: Determination of the Apparent Thickness of the Monolayer by Scanning Tunneling Microscopy	5. FUNDING NUMBERS
6. AUTHOR(S) W. Li, J.A. Virtanen, and R.M. Penner	N00014-93-1-0757

7. PERFORMING ORGANIZATION NAME(S) AND ADDRESS(ES) University of California, Irvine Department of Chemistry Irvine, CA 92717-2025	8. PERFORMING ORGANIZATION REPORT NUMBER Technical Report No. 2
9. SPONSOING/MONITORING AGENCY NAME(S) AND ADDRESS(ES) Office of Naval Research 800 North Quincy Street Arlington, VA 22217	10. SPONSORING/MONITORING AGENCY REPORT NUMBER R&T Number: 400X119YIP

11. SUPPLIMENTARY NOTES

12A. DISTRIBUTION AVAILABILITY STATEMENT Approved for public release, distribution unlimited	12B. DISTRIBUTION CODE

13. ABSTRACT (*Maximum 200 Words*)

The STM is employed to monitor the effect of adsorption of an n-alkanethiolate monolayer, from an aqueous solution of the thiol, on the apparent topography of nanoscopic silver adsorption sites. Silver nano-disk structures were electrochemically deposited on graphite surfaces using the STM. The topography of these adsorption sites was then determined *in-situ* by STM imaging prior to the exposure of the nano-structure to an aqueous solution of an n-alkane thiol. The apparent thickness of the self-assembled monolayer (SAM), estimated from the difference in the nano-structure height measured before and after adsorption of the monolayer, increased linearly with the alkyl chain length for five n-alkane thiols (i.e., $C_nH_{(2n+1)}SH$) having even numbered chain lengths from n=10 to 18. For SAMs of tetradecane thiol, hexadecane thiol, and octadecane thiol, the average height increments equaled the expected all-trans chain length of these molecules indicating that little penetration of the STM tip into the surface of the monolayer occurs during the STM imaging experiment.

14. SUBJECT TERMS STM, n-alkane thiols, biological, lithography, passivation	15. NUMBER OF PAGES 22
	16. PRICE CODE

17. SECURITY CLASSIFICATION OF REPORT Unclassified	18. SECURITY CLASSIFICATION OF THIS PAGE Unclassified	19. SECURITY CLASSIFICATION OF ABSTRACT Unclassified	20. LIMITATION OF ABSTRACT Unlimited

NSN 7540-01-280-5500

Self-Assembly of n-Alkanethiolate Monolayers on Silver Nano-Structures: Determination of the Apparent Thickness of the Monolayer by Scanning Tunneling Microscopy

Wenjie Li, Jorma A. Virtanen, and Reginald M. Penner*

Institute for Surface and Interface Science (ISIS)

Department of Chemistry

University of California, Irvine

Irvine, CA 92717-2025

Abstract: The scanning tunneling microscope (STM) is employed to monitor the effect of adsorption of an n-alkanethiolate monolayer, from an aqueous solution of the thiol, on the apparent topography of nanoscopic silver adsorption sites. Silver nano-disk structures, 1000-1500Å in diameter and 50-150 Å in height, were electrochemically deposited on graphite surfaces using the STM. The topography of these adsorption sites was then determined *in-situ* by STM imaging prior to the exposure of the nano-structure to an aqueous solution of an n-alkane thiol. Immediately following exposure to the thiol, STM images revealed an increase in the height of the nano-structure resulting from the self-assembly of an n-alkane thiolate monolayer on the silver surface. The apparent thickness of the self-assembled monolayer (SAM), estimated from the difference in the nano-structure height measured before and after adsorption of the monolayer, increased linearly with the alkyl chain length for five n-alkane thiols (i.e., $C_nH_{(2n+1)}SH$) having even numbered chain lengths from n=10 to n=18. For SAMs of tetradecane thiol ($CH_3(CH_2)_{13}SH$), hexadecane thiol ($CH_3(CH_2)_{15}SH$), and octadecane thiol ($CH_3(CH_2)_{17}SH$), the average height increments (20Å, 24 Å, and 28Å, respectively) equaled the expected all-trans chain length of these molecules within the experimental precision of our measurement indicating that little penetration of the STM tip into the surface of the monolayer occurs during the STM imaging experiment.

*Author to whom correspondence should be addressed.

Introduction.

Increasingly, the scanning tunneling microscope (STM) is being used to investigate the structure of self-assembled monolayers (SAMs) of n-alkanethiolate molecules on gold and silver surfaces.[1-14] So far, however, it has not been possible to deduce (from STM data alone) the position of the STM tip with respect to the surface of the monolayer during STM imaging as a function of the tunneling conditions. Based on measurements of the electrical conductivity of n-alkanethiolate SAMs on Au(111), and observations of the rate of electron transfer across n-alkanethiolate SAMs to electron donor-acceptor species which are either dissolved in a contacting liquid phase[15] or covalently attached to the SAM,[16-18] it has been concluded that n-alkanethiolate monolayers prepared from long-chain thiols (i.e., $C_nH_{2n+1}SH$, n>10) possesses insufficient conductivity to support even a small STM tunneling current. If this were the case, penetration of the STM tip into the n-alkanethiolate monolayer would be required in order for a stable tunnel junction to be established between the STM tip and the underlying metal surface, and mechanical disruption of the monolayer would result. Under these circumstances, the STM would obviously not be a useful, nonperturbative probe of the monolayer structure. Therefore, the issue of tip penetration may decide the suitability of STM for investigations of the structure of self-assembled monolayers of n-alkane thiols and related adsorbate layers such as Langmuir-Blodgett monolayers and bilayers of long-chain amphiphilic molecules.

To date, the most reliable information regarding the position of the STM tip during tunneling to molecular assemblies, including n-alkanethiolate monolayers, has been gleaned from investigations of these monolayers using instruments which permitted the tip-surface force and the tunneling current to be concurrently measured.[5,7,12] In an investigation by Dürig *et al.*,[12] mercaptohexadecanol (i.e., $HO(CH_2)_{16}SH$) monolayers on Au(111) were probed in ultra-high vacuum (UHV) and it was concluded that the formation of a tunnel junction (with the SAM-covered gold surface) having a resistance

of 10^8 Ω causes an <u>elastic</u> deformation of the monolayer involving a tip penetration of not more than 3Å.[12,19] Likewise, Salmeron et. al.[7] investigated monolayers of $CH_3(CH_2)_{12}SH$ and $CH_3(CH_2)_{22}SH$ on Au(111) in air. During tip-approach experiments in which the force/tunneling probe (with a 100 mV applied bias) was slowly translated toward the monolayer surface, currents in excess of 1.0 µA were detected immediately (i.e. within a few angstroms) upon the detection of tip-monolayer contact via the force measurement.[7] A concurrent STM/AFM investigation by Specht et al.[5] of weakly physisorbed phospholipid bilayers and multilayers - deposited on graphite surfaces using Langmuir-Blodgett techniques - concluded that low voltage (e.g., tip-sample bias $< \pm1.0$ V) tunneling through phospholipid monolayers having a thickness of $\approx$30Å was possible without detectable penetration of the STM tip into the monolayer. Collectively these results are surprising in view of previous concurrent force and tunneling measurements at adsorbate-free surfaces[20-24] which indicated that typical STM tunneling conditions are associated with relatively large tip-sample forces (e.g., 2×10^{-6}N for a 500Å dia. tungsten tip on graphite in air tunneling at 0.5 nA and 40 mV).[23] It is apparent in recent experiments,[7,12] however, that the applied force is distributed over a relatively large tip-surface interfacial contact area ($>$1000Å^2) and that the resulting pressure applied by the tip is smaller than the minimum required for plastic deformation of the surface.

Whereas concurrent force and tunneling measurements provide one experimental approach by which penetration of the STM tip into an n-alkane thiolate monolayer can be detected, another is direct measurement with the STM of the apparent thickness of the monolayer, l_{app}, and comparison of l_{app} with the known or expected monolayer thickness. Here we report the first measurement of l_{app} which was accomplished by preparing SAMs on silver nano-disk structures having diameters of 1000-1500Å and heights of 50-150Å. These adsorption sites were electrochemically synthesized on a highly oriented pyrolytic graphite surfaces using a scanning tunneling

microscope (STM) via a procedure described previously[25,26] The "STM-apparent" thickness of an n-alkanethiolate SAM was obtained by first measuring the average apparent height of a freshly deposited silver nano-disk from *in-situ* STM images of the nano-structure acquired in the silver deposition solution or in pure water. The n-alkanethiolate SAM was then formed by exposure of the silver nano-disk to a dilute aqueous solution of the thiol, and a second series of STM images were acquired from which a new averaged height of the nano-disk was measured. The increase in the average height of the SAM-modified nano-structure following SAM formation equaled l_{app}. Measurements of l_{app} for five thiols $(C_nH_{2n+1}SH)$, having even numbered alkyl chain lengths from n=10 to n=18 (henceforth C_{10} to C_{18}), increased linearly from 12 to 28Å. For the longest three molecules in this series, C_{14}, C_{16}, and C_{18}, l_{app} equaled the calculated thickness of an all-trans n-alkanethiolate monolayer within the experimental precision of the measurement. These data allow the maximum penetration of the STM tip into the monolayer to be estimated at between 3Å (for the C_{18} thiolate SAM) and 6Å (for the C_{14} thiolate SAM). An important and unique advantage of the unusual experimental method employed here is that measurements of the nano-structure height - both before and following formation of a SAM - could be obtained with reference to the atomically smooth graphite surface which was completely unreactive to thiol chemisorption. For this reason, particularly accurate estimates of l_{app} are obtainable for n-alkane thiolate monolayers (and, in principle, other adsorbate layers) using this method.

Experimental Section

Silver nano-disks were grown electrochemically on graphite surfaces using a previously described procedure.[25,26] Briefly, electrochemical growth of silver nanostructures was induced by the application of 6.0 V x 50 µsec (tip-positive) bias voltage pulses between the STM tip and a graphite surface immersed in aqueous

0.5 m$\underline{M}$ AgF (Aldrich, >99.99%). The bias pulse induced the electrochemical growth of a nanoscopic silver adsorption site by a two step mechanism involving the formation of a monolayer-deep pit in the graphite surface within ≈5 μsec of the application of the bias pulse, and the subsequent diffusion-controlled deposition of silver until the termination of the pulse at 50 μsec. The dimensions of the silver nano-structure were controllable either via the bias pulse duration and/or the silver ion concentration.

Following the deposition and *in-situ* characterization of the deposit by STM imaging, the alkane thiol of interest was introduced into the STM using either of two methods: For liquid thiols (n ≤ 16), 20μl of neat thiol was injected into ≈200μl of the aqueous 0.5 m$\underline{M}$ silver plating solution contained in a Kel-F liquid cell in the STM. Following injection, approximately five minutes elapsed before high magnification STM images of the nano-structure were reacquired. Alternatively, n-octadecane thiol - a solid at room temperature - was introduced as a solution in mineral oil using the same technique. Following introduction into the STM electrochemical cell, this mineral solution floated as a thin film on the surface of the aqueous electrolyte in the cell, and partitioning of the n-alkane thiol into the electrolyte occurred. In selected experiments, to insure that silver ion in the contacting electrolyte was not affecting the value of I_{app}, the silver plating solution was first replaced with deionized water prior to the introduction of thiol by either of the methods described above. No difference in the measured values of I_{app} were observed when the SAM was formed in pure water as compared with the 0.5 m$\underline{M}$ AgF plating solution within the precision of the measurement.

Results

For the determination of I_{app}, relatively large silver nano-structures having diameters greater than 1000Å were employed as adsorption sites in order to minimize the effect of curvature of the silver surface on the ordering of molecules in an adsorbate layer. A typical nano-structure employed in this study is shown in the STM image of

Fig. 1A. The height of the nano-structure is rendered with a magnification 2.6 times greater than the lateral (or x and y-) dimensions to accentuate the detailed topography of the structure. As shown in the cross-sections of Fig. 2A, the diameter and height of the nano-structure are $\approx$1500Å and $\approx$100 Å, respectively. Excluding the outer-most 100Å at the edge of the disk (where the height of the structure is increasing rapidly) the root mean square roughness of the surface is 8Å. Figure 1B shows the same silver adsorption site following exposure to tetradecane ($C_{14}H_{29}SH$). An increase in height (from an average of 99Å to 125Å) is evident in both the STM image, and a cross-section of the nano-structure, shown in Fig. 2B. Whereas this STM image was acquired using an imaging bias of 40 mV (tip-positive) and a current of 0.6 nA, the apparent height of this nano-structure was unchanged for currents in the interval from 0.2 nA to 0.8 nA. For tunneling currents in excess of 0.9 nA, the nano-structure height became irreproducible but smaller, on average, than in STM images acquired at lower currents. These high-current STM images of the nano-structure also exhibited much greater noise.

Shown in Figure 3 is the time dependence of the averaged nano-structure height and volume for the silver feature shown in Figure 2, calculated from a series of STM images acquired both before exposure to thiol and after. In the particular case of this nano-structure, some erosion of the height and volume was observed just prior to the exposure to tetradecane thiol. In our experience, this instability is unusual for silver nano-structures in dilute silver-ion containing solutions when the STM imaging bias is small (E_B < 30 mV) and sample-negative. It is apparent from Fig. 3 that exposure of the silver nano-disk to thiol and formation of the SAM immediately stabilized the nano-structure, and the new height after adsorption was unaffected by repetitive STM imaging with a tip-bias of +40 mV and a tunneling current of 0.8 nA. The exploitation of n-alkanethiolate SAMs to stabilize metal nano-structures under conditions where they are demonstrably unstable (e.g. at sample-positive biases) has been described.[27] As already noted, the step-wise increase in height of the silver nano-structure which is

apparent following the introduction of the n-alkanethiol molecules to the solution equals 26Å. In the discussion which follows, this incremental height increase is equated with I_{app}.

Values of I_{app} were measured for SAMs composed of four other n-alkane thiols (decane thiol (C_{10}), dodecane thiol (C_{12}), hexadecane thiol (C_{16}), and octadecane thiol (C_{18})) using the same procedure: Synthesis of a nanoscopic silver adsorption site, exposure of the nano-structure to the thiol of interest, and measurement of the incremental increase in nano-structure height following SAM formation using the STM. Irrespective of the alkyl chain length, reproducible measurement of the nano-structure height following SAM formation was possible using a tunneling current in the interval from 0.2 nA to 0.8 nA and imaging biases near 40 mV (tip-positive). No observable changes in the height of the SAM-modified nano-structure were observable over this range of currents however larger currents resulted in increased noise and generally irreproducible results for the nano-structure height. Tunneling currents smaller than approximately 0.1 nA were inaccessible in these *in-situ* STM imaging experiments due to the presence of noise resulting from background faradaic current signal having an average amplitude of ≈10-20pA. Likewise, biases larger than 100 mV caused an appreciable increase in the Faradaic current and it was therefore not possible to probe the effect of bias on the apparent height of the SAM-modified silver nano-structures in this study. Measurements of I_{app} for five n-alkane thiols having even number alkyl chains ranging in length from C_{10} to C_{18} are summarized in Figure 4. A linear increase in I_{app} with alkyl chain length was observed ranging from 12Å for decanethiolate (C_{10}) to 28Å for octadecanethiolate (C_{18}). Least squares analysis of these experimental data yields a slope of 1.85 Å/methylene and an intercept of -6.9Å (*vide infra*).

Discussion.

The schematic diagram shown in Figure 5 illustrates the various heights which are relevant to the measurement of l_{app} described in this paper. Prior to SAM formation, the *apparent* height of a silver nano-structure, $h_{app,1}$, equals the sum of the true height of the nano-structure (d_{silver}), and the difference between the two tunneling distances which apply when the tip is located above the silver nano-structure ($d_{tunneling,Ag}$) and above the bare graphite surface ($d_{tunneling,HOPG}$):

$$h_{app,1} = d_{silver} + (d_{tunneling,Ag} - d_{tunneling,HOPG}) \tag{1}$$

Following exposure to the n-alkane thiol, the true STM-apparent thickness of the SAM, l^o_{app}, provides an additional contribution to the apparent height measured from the graphite surface:

$$h_{app,2} = (d_{silver} + l^o_{app}) + (d_{tunneling,SAM} - d_{tunneling,HOPG}) \tag{2}$$

where $d_{tunneling,SAM}$ is the tunneling distance when the tip is located above the SAM-modified silver nano-structure. The difference in height, $\Delta h_{app} = h_{app,2} - h_{app,1}$, is defined here as the STM-apparent thickness of the SAM, l_{app}:

$$l_{app} = l^o_{app} + (d_{tunneling,SAM} - d_{tunneling,Ag}) \tag{3}$$

The interpretation of the STM data for clean and SAM-modified silver nano-structures presented next assumes that $l_{app} \approx l^o_{app}$ and, therefore, that $d_{tunneling,SAM} \approx d_{tunneling,Ag}$ for identical conditions of tip-sample bias and tunneling current.

In Figure 4, measured values of l_{app} for monolayers prepared from the five thiol molecules are compared with two sets of calculated thickness data: The dashed line in

Fig. 4 (labeled "all-trans") represents the thickness expected for monolayers in which alkane chains have an all-trans conformation. The slope of is line is 1.26 Å/methylene which assumes that molecules in the monolayer possess an average orientation perpendicular to the plane of the surface (i.e., tilt angle = 0°). If a tilt angle of 13° is instead assumed, as estimated for n-alkanethiolate monolayers on evaporated silver surfaces using FTIR and ellipsometry[28,29], and surface-enhanced Raman scattering (SERS)[30], the slope of this line decreases slightly to 1.23Å/methylene. The intercept of the dashed line of 3.6Å is required to accommodate the length of the -S-Ag moiety and is also consistent with the experimental observations of Walczak et al.[28]

The dotted line in Figure 4 (labeled "liquid crystalline") has a slope of 0.86Å/methylene and the same intercept of 3.6Å as the "all-trans" line. The weaker dependence of the monolayer thickness on alkyl chain length is obtained from the experimental x-ray diffraction data of Lewis and Engelman[31] for liquid crystalline phase_-phosphatidylcholine (PC) bilayers at temperatures above the chain-melting transition. The slope of 0.86Å/methylene was obtained for a series of five PCs having saturated, even numbered alkyl chains ranging in length from C_{10} to C_{18}. As compared with the prediction for all-trans alkyl chains, the smaller slope of the Lewis and Engelman data is consistent with what is known about conformational disorder in crystalline n-alkane phases. Investigations of melting and pre-melting phenomena for crystalline n-alkanes by FTIR[32,33] have determined that conformational disorder usually takes the form of gauche defects at the methyl terminus (so called "end-gauche" defects) and "kinked" alkyl chains resulting from two gauche bonds arranged in a gauche-trans-gauche sequence near the methyl terminus.[32-34] The net effect of a single end-gauche defect or kink is to reduce the total length of the molecule by approximately one methyl increment as compared with the all-trans chain. Furthermore, the probability of finding either type of defect in an alkyl chain increases linearly with the chain length.[33] The

0.86Å/methylene slope observed by Lewis and Engelman[31] is a manifestation of these two effects.

Good agreement is obtained in Figure 4 between the predicted "all-trans" monolayer thickness and the experimentally measured values of l_{app} for the longest three thiols in this study: C_{14}, C_{16}, and C_{18}. The l_{app} values for these three molecules were 20Å, 24Å, and 28Å, respectively, with a standard deviation for each thickness value of approximately 4Å. The predicted "all-trans" thicknesses are 21.2Å, 23.8Å, and 26.3Å for monolayers of these three molecules. The implication of this agreement is that little or no penetration of the SAM by the STM tip occurs during the STM imaging of these monolayers. This conclusion follows from the fact that the measured position of the STM tip above the silver surface during imaging of the monolayer, l_{app}, nearly coincides with the largest possible monolayer thickness which is equal to the all-trans prediction shown in Figure 4. However, while no penetration of the SAM by the STM tip is required to account for the data of Fig. 4, the uncertainty in these measurements permit a maximum tip penetration of between 3Å (for the C_{18} thiolate SAM) and 6Å (for the C_{14} thiolate SAM).

For SAMs of the shortest two molecules investigated in this study, C_{10} and C_{12}, the measured values of l_{app} (12Å and 15Å, respectively) are significantly smaller than the predicted all-trans monolayer thicknesses of 16.2 Å and 18.7 Å. While the origin of this disparity can not be resolved from the experimental data, two explanations may be advanced. The first possibility is that the experimental measurement reflects the true thickness of these monolayers, and that these monolayers exhibit a reduced thickness as a consequence of the existance of gauch defects in the alkyl chains. As already noted, the presence of a single g-t-g defect (where the trans (t) segment may be any number of methylenes in length) decreases the monolayer thickness by one methylene unit or 1.26Å. It is well-established (from trends of the chain melting temperature versus chain length for n-alkanes, for example) that the total cohesive energy between n-alkyl

chains varys directly with chain length which, in turn, is correlated with the chain melting temperature. For the crystalline α phase of long chain n-alkanes (in which n-alkyl chains are arranged in a lamellar crystal; similar to the n-alkane chains in thiolate monolayers) the chain melting transition, T_m, for C_{13} is 5°C whereas for C_{19}, T_m = 32°C.[35] Based on these numbers, the expectation is that monolayers of the C_{10} and C_{12} thiols are likely liquid crystalline at room temperature (and therefore significantly disordered) whereas the C_{18} and C_{20} monolayers are crystalline at this temperature. This picture is corroborated by IR spectroscopic investigations of n-alkanethiolate monolayers on polycrystalline gold surfaces by Porter et al.[15] Following a detailed examination of the CH_2 stretching region, these authors conclude that monolayers of n-alkane thiols which are C_{16} or shorter are liquid crystalline, and that monolayers of longer thiols (up to C_{22} in this study) are crystalline.[15] The data for l_{app} versus chain length plotted in Figure 4, therefore, is entirely consistant with this picture.

However, based solely on the experimental evidence, we can not discount the possibility that the C_{10} and C_{12} monolayers are all-trans - not liquid crystalline. In this case, the disparity between the all-trans thickness and the measured l_{app} values for these monolayers must derive from a penetration of the STM tip into the monolayer of between 1Å and 6Å. The existence of significant tip penetration for the C_{10} and C_{12}, however, is surprising since the conductivity of the thinner monolayers are predicted to be higher than the conductivity of monolayers of the C_{18} and C_{20} thiols. For example, based on β values recently reported by Jordan et al.[36,37] for diethynylalkanes, the C_{12} n-alkyl chain is expected to have a conductivity more than twice as high as a C_{18}.[38] In addition, STM images of C_{10} or C_{12} thiol-modified silver nanostructures provide no indication of modifications to the monolayer surface (e.g. "furrowing" along the fast scan direction) which might be indicative of tip penetration into the monolayer while scanning. However the arguements advanced in the previous paragraph suggest that monolayers of the shorter C_{10} and C_{12} are nearer their respective chain melting transitions (if these

monolayers are somehow all-trans at room temp.) and therefore can be expected to exhibit greater susceptibility to tip pentration than monolayers of the longer C_{18} and C_{20}.

Summary

We describe a new method for deducing the position of an STM tip relative to a metal surface during STM imaging of an adsorbate-covered metal surface. This method involves the *in-situ* formation of a metal adsorption site, and the measurement by STM of the adsorption site height before and following formation of an adsorbate monolayer on the metal surface. Adsorption sites having suitable dimensions and an acceptible roughness are readily generated using an *in-situ* metal deposition procedure reported earlier. We believe that particularly accurate measurements of the apparent thickness of an adsorbate monolayer are possible using this procedure because the nanostructure _ height measurement is referenced to the level of the atomically smooth and chemically inert graphite surface on which the metal adsorption site is supported.

Using this strategy, *in-situ* STM measurements of the apparent n-alkanethiolate monolayer thickness on silver nanostructures have been performed. The measured thicknesses equal the predicted all-trans thickness of the monolayer for SAMs prepared from n-alkanethiols having alkane chain lengths of C_{14}, C_{16}, and C_{18} within the experimental precision of our measurement. These data allow the <u>maximum</u> penetration depth of the STM tip into the surface of the monolayer to be estimated at between 3Å (for the C_{18} thiolate SAM) and 6Å (for the C_{14} thiolate SAM). Significantly, these data are also entirely consistant with no penetration of the monolayer by the STM tip, in qualitative agreement with the concurrent force and tunneling measurements on similar systems reported previously. For thinner monolayers composed of C_{10} and C_{12} thiols, our measurements indicate an STM-apparent thickness which is significantly smaller than the expected all-trans thickness for these monolayers. The observed

disparity may derive either from monolayers which are significantly disordered, or from penetration of these thinner monolayers by the STM tip (to a depth of between 1Å and 6Å) for reasons which are not apparent. Collectively, these results provide reason for optimism regarding the prospects for nonperturbative STM imaging of self-assembled monolayers using the scanning tunneling microscope.

References and Notes

(1) Widrig, C. A.; Alves, C. A.; Porter, M. D. *J. Am. Chem. Soc.* **1991**, *113*, 2805.

(2) Sun, L.; Crooks, R. M. *J. Electrochem. Soc.* **1991**, *138*, L23.

(3) Sun, L.; Crooks, R. M. *Langmuir* **1993**, *9*, 1951.

(4) Stranick, S. J.; Weiss, P. S.; Parikh, A. N.; Allara, D. L. *J. Vac. Sci. Technol. A* **1994**, *11*, 739.

(5) Specht, M.; Ohnesorge, F.; Heckl, W. M. *Surf. Sci. Lett.* **1991**, *257*, L653.

(6) Ross, C. B.; Sun, L.; Crooks, R. M. *Langmuir* **1993**, *9*, 632.

(7) Salmeron, M.; Neubauer, G.; Folch, A.; Tomitori, M.; Ogletree, D. F.; Sautet, P. *Langmuir* **1993**, *9*, 3600.

(8) McCarley, M. L.; Dunaway, D. J.; Willicut, R. J. *Langmuir* **1993**, *9*, 2775.

(9) Kim, Y. T.; Bard, A. J. *Langmuir* **1992**, *8*, 1096.

(10) Kim, Y. T.; McCarley, R. L.; Bard, A. J. *J. Phys. Chem.* **1992**, *96*, 7416.

(11) Edinger, K.; Gölzhäuzer, A.; Demota, K.; Wöll, C.; Grunze, M. *Langmuir* **1993**, *9*, 4.

(12) Dürig, U.; Züger, O.; Michel, B.; Häussling, L.; Rigsdorf, H. *Phys. Rev.B* **1993**, *48*, 1711.

(13) Häussling, L.; Michel, B.; Rigsdorf, H.; Rohrer, H. *Angew. Chem. Int. Ed. Engl.* **1991**, *30*, 569.

(14) Chailapakul, O.; Sun, L.; Xu, C.; Crooks, R. M. *J. Am. Chem. Soc.* **1993**, *115*, 12459.

(15) Porter, M. D.; Bright, T. B.; Allara, D. L.; Chidsey, C. E. D. *J. Am. Chem. Soc.* **1987**, *109*, 3559.

(16) Chidsey, C. E. D. *Science* **1991**, *251*, 919.

(17) Finklea, H. O.; Hanshew, D. D. *J. Am. Chem. Soc.* **1992**, *114*, 3173.

(18) Finklea, H. O.; Ravenscroft, M. S.; Snider, D. A. *Langmuir* **1993**, *9*, 223.

(19) Siepmann, J. I.; McDonald, I. R. *Phys. Rev. Lett.* **1993**, *70*, 453.

(20) Dürig, U.; Gimzewski, J. K.; Pohl, D. W. *Phys. Rev. Lett.* **1986**, *57*, 2403.

(21) Martin, Y.; Wickramasinghe, H. K. *Appl. Phys. Lett.* **1987**, *50*, 1455.

(22) Mate, C. M.; Erlandsson, R.; McClelland, G. M.; Chiang, S. *Surf. Sci.* **1989**, *208*, 473.

(23) Tang, S. L.; Bokor, J.; Storz, R. H. *Appl. Phys. Lett.* **1988**, *52*, 188.

(24) Yamada, H.; Fujii, T.; Nakayama, K. *J. Vac. Sci. Technol. A* **1988**, *6*, 293.

(25) Li, W.; Virtanen, J. A.; Penner, R. M. *Appl. Phys. Lett.* **1992**, *60*, 1181.

(26) Li, W.; Virtanen, J. A.; Penner, R. M. *J. Phys. Chem.* **1992**, *96*, 6529.

(27) Li, W.; Virtanen, J. A.; Penner, R. M. *Langmuir* submitted for publication.

(28) Walczak, M. M.; Chung, C.; Stole, S. M.; Widrig, C. A.; Porter, M. D. *J. Am. Chem. Soc.* **1991**, *113*, 2370.

(29) Laibinis, P. E.; Whitesides, G. M.; Allara, D. L.; Tao, Y. T.; Parikh, A. N.; Nuzzo, R. G. *J. Am. Chem. Soc.* **1991**, *113*, 7152.

(30) Bryant, M. A.; Pemberton, J. E. *J. Am. Chem. Soc.* **1991**, *113*, 8284.

(31) Lewis, B. A.; Engelman, D. M. *J. Mol. Biol.* **1983**, *166*, 211.

(32) Kim, Y.; Strauss, H. L.; Snyder, R. G. *J. Phys. Chem.* **1989**, *93*, 7520.

(33) Maroncelli, M.; Strauss, H. L.; Snyder, R. G. *J. Chem. Phys.* **1985**, *82*, 2811.

(34) Kim, Y.; Strauss, H. L.; Snyder, R. G. *J. Phys. Chem.* **1988**, *92*, 5080.

(35) Broadhurst, G. *J. Res. Natl. Bur. Stand. Sect. A* **1962**, *66*, 241.

(36) Shephard, M. J.; Paddon-Row, M. N.; Jordan, K. D. *Chemical Physics* **1993**, *176*, 289.

(37) Paddon-Row, M. N.; Shephard, M. J.; Jordan, K. D. *J. Phys. Chem.* **1993**, *97*, 1743.

(38) Considered two molecules: $D-(CH_2)_x-A$ and $D-(CH_2)_{x+n}-A$ where (D) is an electron donor moiety, (A) is an electron acceptor moiety, and (n) is the difference in length in the all-trans alkyl spacer in terms of the number of sigma bonds. For these two molecules, the unimolecular rate constants for electron transfer can be related through the expression: $k_2 = k_1 exp(-\beta n)$ where k_1 and k_2 are the rate constants for the shorter and longer bridges, respectively. β has been calculated[37] as a function

of spacer length in 2-sigma bond increments for all-trans polymethylene chains (in model molecules in which both D and A are ethynyl moieties) with the following results: $\beta_{12/14} = 0.14$, $\beta_{14/16} = 0.13$, and $\beta_{16/18} = 0.12$. The ratio k_2/k_1 is therefore obtained from the expression: $k_2/k_1 = \exp(-2(\beta_{12/14}+\beta_{14/16}+\beta_{16/18})) = 0.46$. According to this analysis (and to a first approximation) the C_{12} is expected to exhibit an electronic conductivity which is a factor of $\approx 0.46^{-1}$ greater than the C_{18}. For the other electron donor and acceptor moieties and spacer conformations considered by the authors, the calculated β values were larger.

Figure Captions

Figure 1 - STM images of a silver nano-structure electrochemically deposited on a graphite surface: **A.** The silver nano-structure is shown immediately following deposition in an aqueous solution of 0.5 m$\underline{M}$ AgF. **B.** The same nano-structure is shown following the addition of n-tetradecane thiol to this solution. Both images were acquired using an imaging bias, E_B = 40 mV (tip-positive) and a tunneling current of 0.6 nA.

Figure 2 - Cross sections of the silver nanostructures shown in Figure 1 before (**A.**), and, immediately following (**B.**), exposure to n-tetradecane thiol.

Figure 3 - Plot of the average height of the silver nano-structures shown in Figures 1 and 2 as a function of time calculated from STM images acquired both before and following the addition of n-tetradecane thiol.

Figure 4 - Schematic diagrams depicting a cross-sectional view of a silver nano-structure before (**A.**) and following (**B.**) self-assembly of an n-alkanethiolate monolayer on the surface of the silver nanostructure. Contributions to the STM-apparent height of the nano-structure, l_{app} , are indicated and are discussed in the text.

Figure 5 - A plot of the apparent thickness of the n-alkanethiolate monolayer versus the length of the n-alkane chain for a series of five n-alkane thiols. In this plot, the predicted thickness for an all-trans monolayer having 0° chain tilt from the surface normal is shown by the dashed line and the predicted thickness for a liquid-crystalline monolayer is shown by the dotted line (*vide infra*).

A.

200Å
100Å
0Å

400 nm

200 nm

0 nm

400 nm   200 nm   0 nm

B.

200Å
100Å
0Å

400 nm

200 nm

0 nm

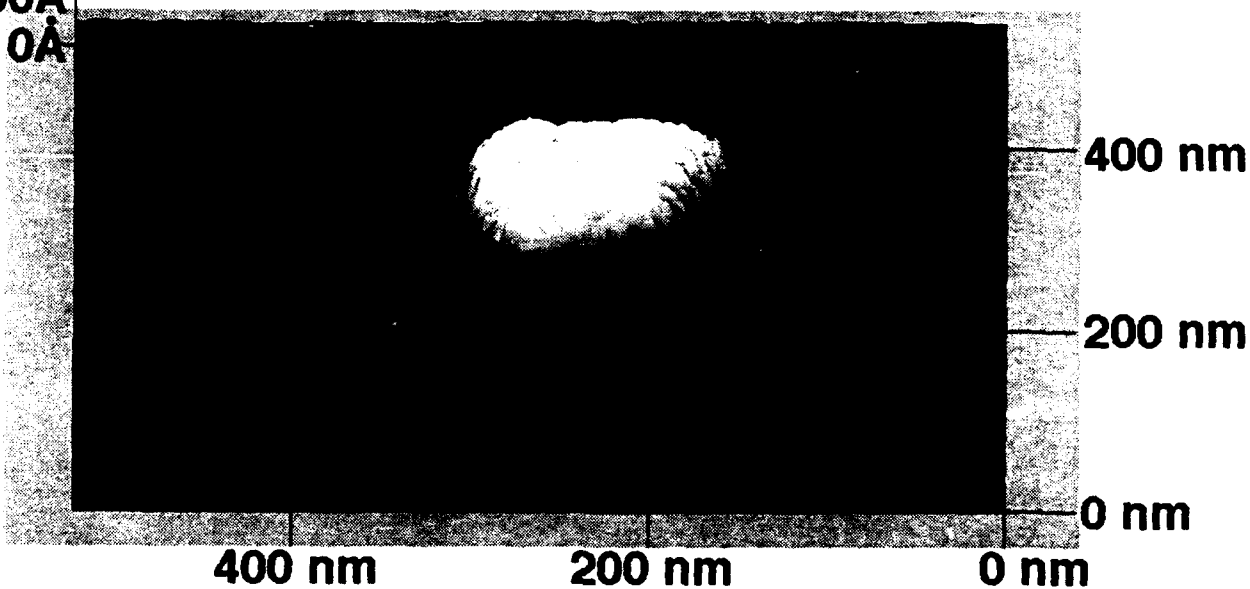400 nm   200 nm   0 nm
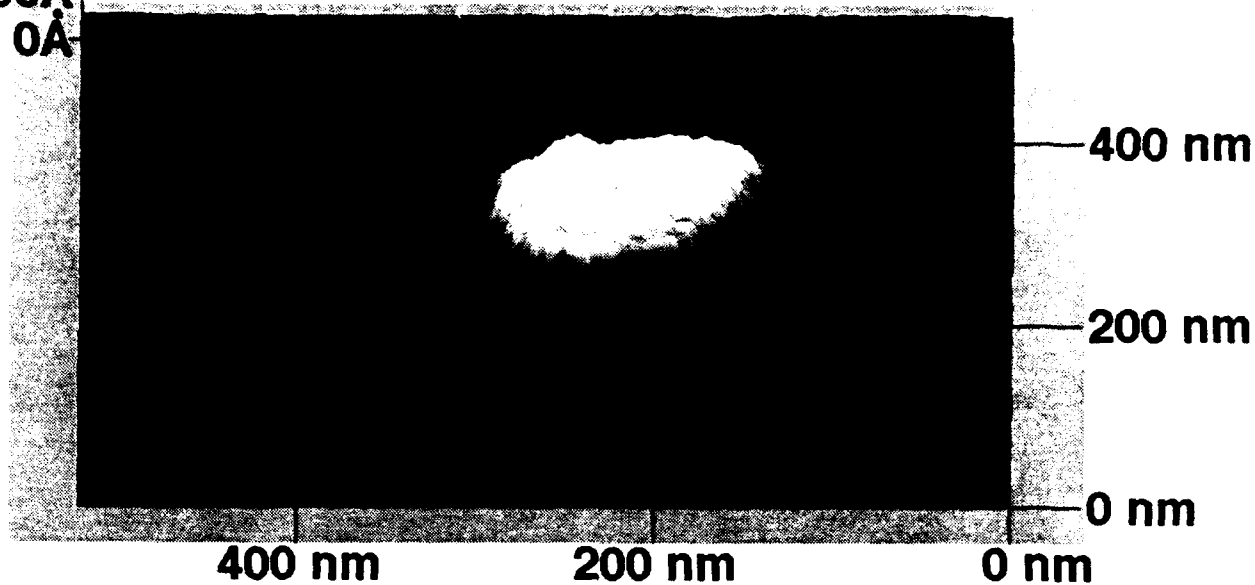
Figure 1. Li *et al.*, ISIS, Dept. of Chem., UC Irvine
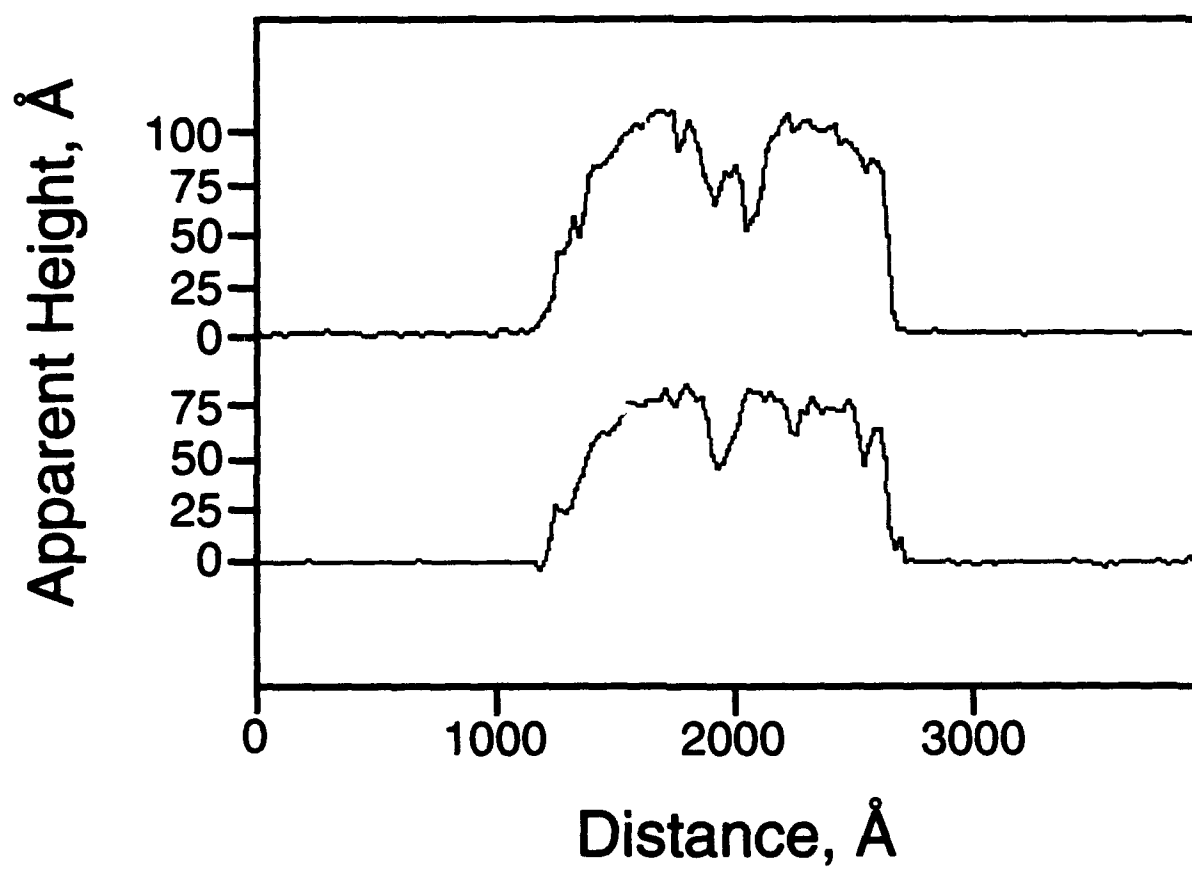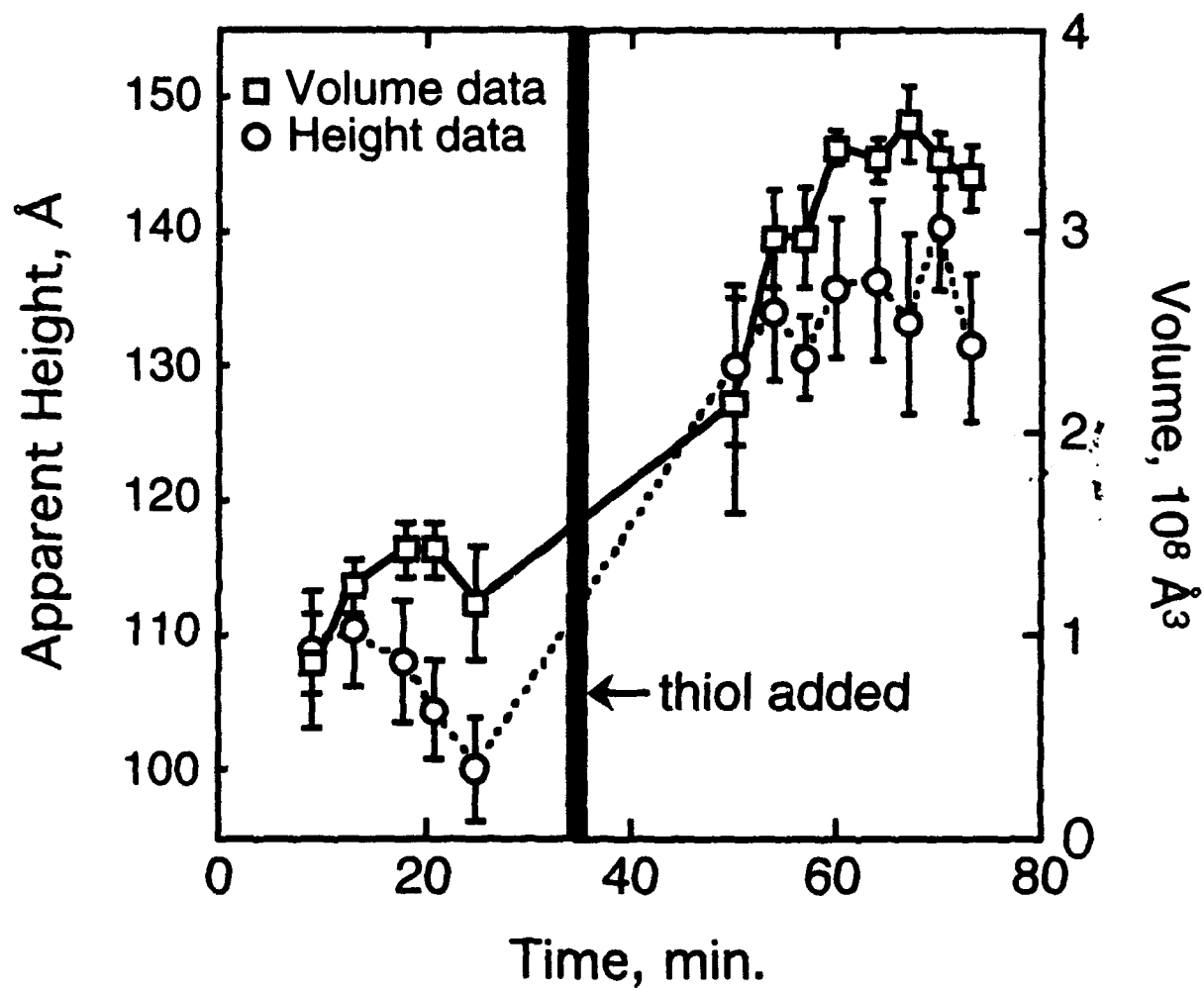
Figure 2. Li *et al.*, ISIS, Dept. of Chem., UC Irvine
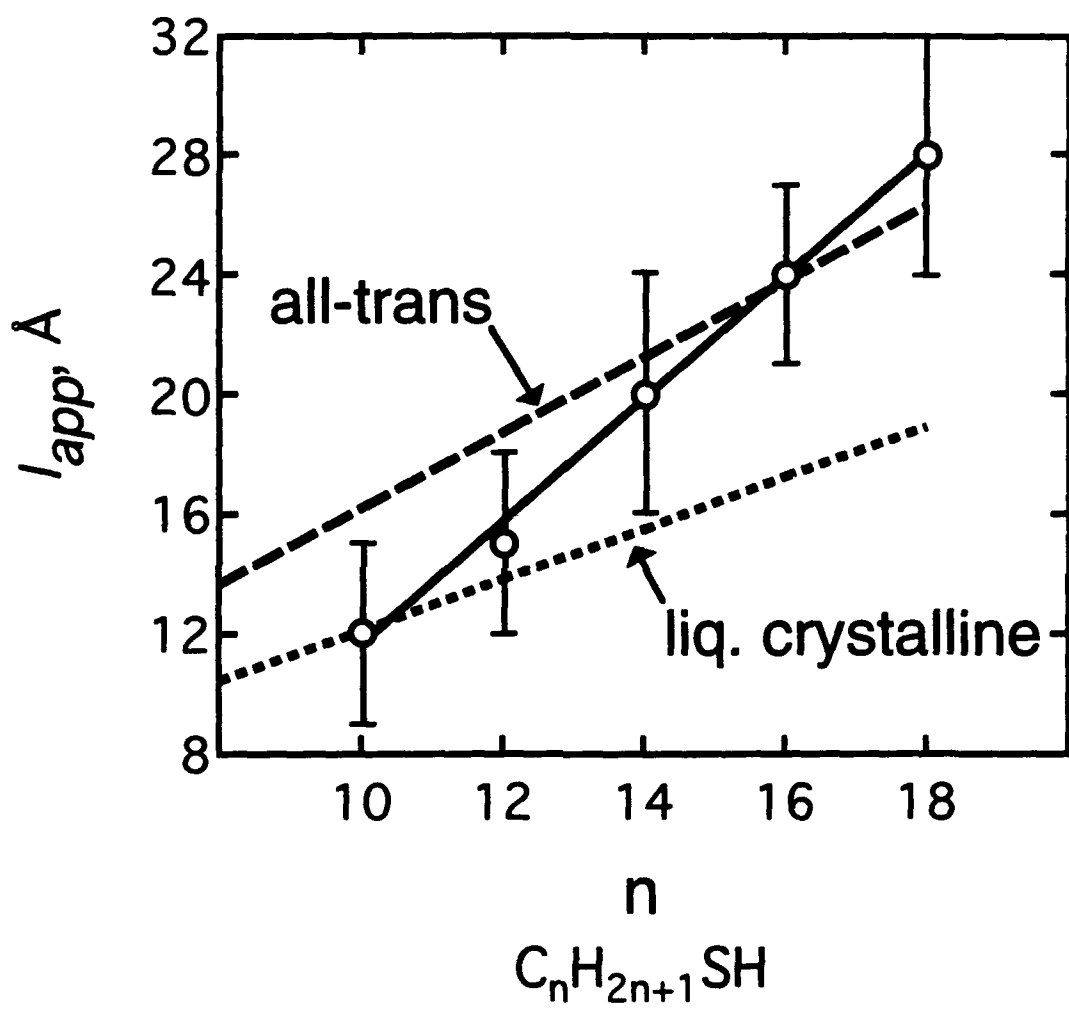
Figure 3. Li et al., ISIS, Dept. of Chem., UC Irvine

Figure 4. Li *et al.*, ISIS, Dept. of Chem., UC Irvine

A. insulated STM tip — Aq. 0.5 m$\underline{M}$ AgF — $d_{tunneling,HOPG}$ — Pt — $h_{app,1}$ — silver — graphite — $d_{tunneling,Ag}$ — d_{silver}

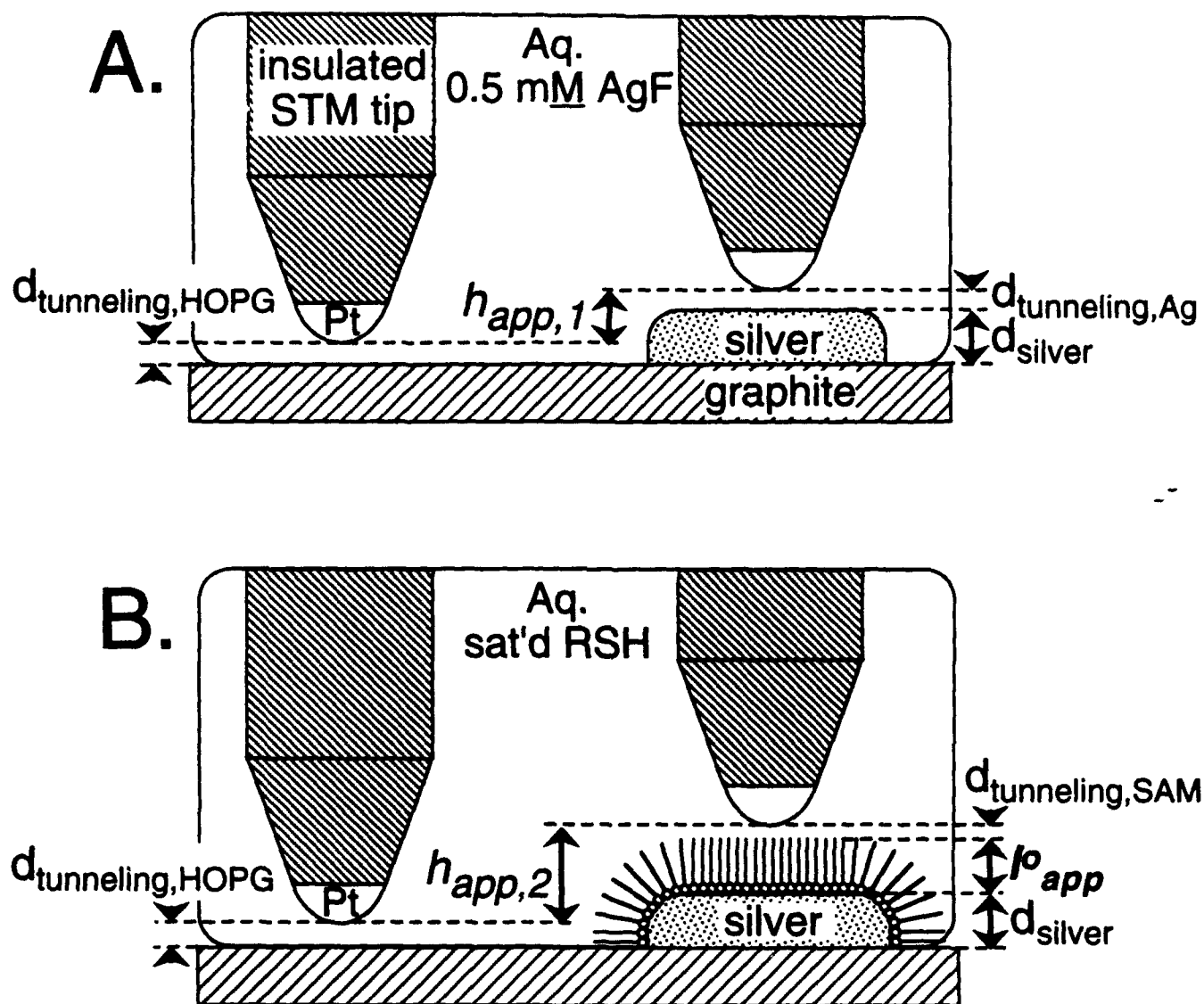**B.** Aq. sat'd RSH — $d_{tunneling,HOPG}$ — Pt — $h_{app,2}$ — silver — $d_{tunneling,SAM}$ — l^o_{app} — d_{silver}

Figure 5. Li *et al.*, ISIS, Dept. Chemistry, UC Irvine